Persistent Anti-Correlations in Brownian Dynamics Simulations of Dense Colloidal Suspensions Revealed by Noise Suppression

Suvendu Mandal,[1] Lukas Schrack,[2] Hartmut Löwen,[1] Matthias Sperl,[3,4] and Thomas Franosch[2]
[1]*Institut für Theoretische Physik II: Weiche Materie, Heinrich-Heine-Universität Düsseldorf, Universitätsstraße 1, 40225 Düsseldorf, Germany*
[2]*Institut für Theoretische Physik, Universität Innsbruck, Technikerstraße 21A, A-6020 Innsbruck, Austria*
[3]*Institut für Materialphysik im Weltraum, Deutsches Zentrum für Luft- und Raumfahrt, 51170 Köln, Germany*
[4]*Institut für Theoretische Physik, Universität zu Köln, Zülpicher Straße 77, 50937 Köln, Germany*

(Received 24 April 2019; revised manuscript received 28 August 2019; published 15 October 2019)

Transport properties of a hard-sphere colloidal fluid are investigated by Brownian dynamics simulations. We implement a novel algorithm for the time-dependent velocity-autocorrelation function (VACF) essentially eliminating the noise of the bare random motion. The measured VACF reveals persistent anti-correlations manifested by a negative algebraic power-law tail $t^{-5/2}$ at all densities. At small packing fractions the simulations fully agree with the analytic low-density prediction, yet the amplitude of the tail becomes dramatically suppressed as the packing fraction is increased. The mode-coupling theory of the glass transition provides a qualitative explanation for the strong variation in terms of the static compressibility as well as the slowing down of the structural relaxation.

DOI: 10.1103/PhysRevLett.123.168001

Introduction.—In a fluid the velocity autocorrelation function (VACF) in equilibrium encodes the self-diffusion coefficient as its time-integral, similar Green-Kubo relations exist for all transport coefficients such as viscosity or heat conductivity [1]. For underlying Newtonian dynamics it is well established since the late 1960s by the pioneering simulations of Alder and Wainwright [2], exact theoretical results [3,4], and experiments [5–8] that the VACF and other relevant correlation functions display an algebraic power-law decay $t^{-3/2}$ in 3D. Such tails then imply a nonanalytic behavior for the frequency-dependent transport coefficients. The origin of these persistent correlations is traced back to the slow diffusion of conserved transverse momentum [1,2,9,10]. Similar tails also arise due to the presence of boundaries [6,11,12] or in the presence of disorder [13–15] or even driven granular systems [16].

For a colloidal suspension, velocity is not an observable anymore, rather it fluctuates without bounds, momentum is lost incessantly due to friction and gained by thermal noise. Nevertheless, a VACF $Z(t)$ can be defined formally by

$$Z(t) := \frac{1}{6}\frac{d^2}{dt^2}\langle[\mathbf{R}(t)-\mathbf{R}(0)]^2\rangle, \qquad t>0, \qquad (1)$$

thereby extending the connection with the mean-square displacement also to the colloidal case. Recently, there has been experimental progress to monitor with high precision the VACF of an isolated colloid in a solvent held by an optical trap [5–8] and confirm that the coupling to the solvent gives rise to long-time tails as above and colored noise as predicted theoretically [17,18].

In Brownian dynamics (BD) the solvent is treated only implicitly by Gaussian white noise and friction, correspondingly these hydrodynamic tails due to momentum conservation do not occur. Yet, exact low-density expansions [19–21] developed in the early 1980s of the many-body Smoluchowski equation in 3D predict a similar long-time behavior for the VACF, although more rapidly decaying $t^{-5/2}$ and with negative prefactor. The tails arise due to particle conservation and reflect the repeated encounters with the same scatterer. Roughly speaking, the particle "remembers" that a second colloid is blocking the way in the relative motion, the constraint fading away only slowly by diffusion. Generally, these tails appear as a universal feature of strongly interacting particle systems lacking momentum conservation. In contrast to the hydrodynamic tails, there appears to be only rudimentary data analysis [22] of BD simulation results to corroborate the persistent tails. The difficulty in obtaining accurate results in BD simulations is that the mean-square displacement is dominated by the white noise keeping the dynamics in equilibrium. For dilute systems the interactions leading to deviations from conventional diffusion are rare events and get buried completely in the noise. For higher packing fractions there is a significant suppression of the diffusive motion, yet the persistent tails (if they prevail beyond the low-density regime) are again hard to extract from noisy data.

In this Letter we present BD simulation data for the VACF over several orders of magnitude in time and amplitude, thereby confirming the existence of such long-time tails for the first time. The key ingredient is an adaption of an algorithm originally introduced by Frenkel [13] for a single

particle on a lattice. At the lowest packing fractions φ the data are fully described by the low-density expansion, in particular we reproduce the short-time divergence as well as the predicted long-time tail. We show that the mode-coupling theory (MCT) of the glass transition for colloids also yields a long-time tail provided the long-wavelength dynamics is properly resolved. The trends in the amplitude of the tail in the simulation are rationalized within MCT. Furthermore, we elaborate the MCT prediction for the VACF in the vicinity of the glass transition.

Model and simulation.—To unravel the VACF in detail, we investigate a hard-sphere colloidal fluid with particles of identical diameters σ and short-time diffusion coefficient D_0 at packing fraction $\varphi = n\sigma^3\pi/6$ [1]. Correspondingly, $t_0 = \sigma^2/D_0$ sets the basic unit of time, $Z(t)\sigma^2/D_0^2$ is the dimensionless VACF. We rely on event-driven Brownian dynamics simulations [23–26] for 1000 particles using a fixed Brownian time step and evolve the particles ballistically including collisions.

Yet, for low densities most of the time no collisions occur and the dynamics is dominated by the noise of the free Brownian motion. Motivated by Frenkel [13], we propose a novel method, which generates two trajectories for an *identical* noise history, one with collisions and another for free Brownian motion ignoring interactions. Accordingly, we split the total displacement of a particle into two contributions

$$\Delta\mathbf{R}(t) = \Delta\mathbf{R}_0(t) + \delta\mathbf{R}(t), \tag{2}$$

where $\Delta\mathbf{R}_0(t)$ represents the random displacement of the noninteracting trajectory. The difference $\delta\mathbf{R}(t)$ is then the collision-induced displacement. Then the mean-square displacement evaluates to

$$\langle\Delta\mathbf{R}(t)^2\rangle = 6D_0t - \langle\delta\mathbf{R}(t)^2\rangle + 2\langle\Delta\mathbf{R}(t)\cdot\delta\mathbf{R}(t)\rangle. \tag{3}$$

The mean-square displacement (MSD) is evaluated for packing fractions ranging from the dilute regime, $\varphi = 0.005$, to just below the freezing transition, $\varphi = 0.48$, see Fig. 1. Both the short-time diffusive motion $\langle\Delta\mathbf{R}(t)^2\rangle = 6D_0t, t \to 0$, as well as the long-time diffusion $\langle\Delta\mathbf{R}(t)^2\rangle = 6D^{(s)}t, t \to \infty$ is properly resolved. From the data we extract the long-time self-diffusion coefficient $D^{(s)}$ and observe a slowing down by a factor of ≈ 7 with respect to the free motion. The crossover regime extends over two decades for the highest densities but appears to be a featureless smooth interpolation.

Clearly, for low densities, the correction terms become small relative to the bare diffusion term by construction. Yet, the simulations reveal that the cross-correlation term $2\langle\Delta\mathbf{R}(t)\cdot\delta\mathbf{R}(t)\rangle$ in the MSD is at least by two orders of magnitude smaller than the correction term $\langle\delta\mathbf{R}(t)^2\rangle$, see Fig. 1(b). We have checked that this hierarchy of contributions persists to all densities. This observation suggests

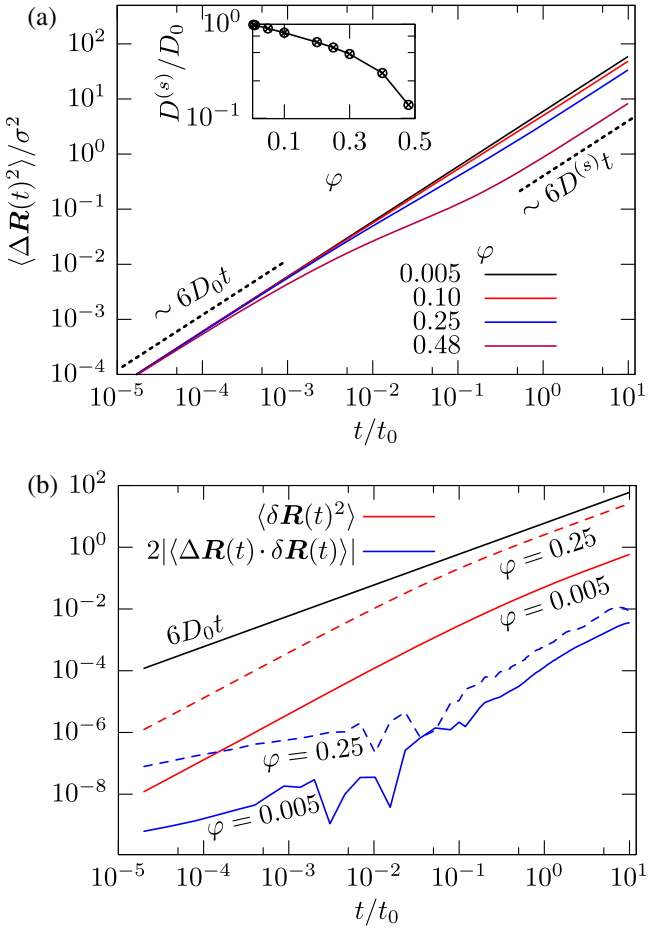

FIG. 1. (a) Mean-square displacement $\langle\Delta\mathbf{R}(t)^2\rangle$ of monodisperse Brownian hard spheres for various packing fractions φ. Inset: Long-time diffusion coefficients $D^{(s)}$ vs packing fraction. (b) Each term in Eq. (3) for packing fractions $\varphi = 0.005$ (solid lines) and $\varphi = 0.25$ (dashed lines).

that we can ignore the cross-correlation completely. Then the collision-induced mean-square displacement captures the suppression of diffusion, reflecting that interaction can only slow down the MSD.

Upon taking derivatives in Eq. (3), the bare diffusion term drops out for $t > 0$ while it formally yields a contribution $6D_0\delta(t)$ at the time origin. The remaining terms can be differentiated numerically and yield high-accuracy data for the VACF. Note that in the low-density regime $\delta\mathbf{R}(t)$ evaluates to zero most of the time, since few collisions occur. Using the observation that the cross-correlation can be ignored, a noise suppression by more than two orders of magnitude is achieved at low densities, see Supplemental Material [27].

The computed VACF reveal nontrivial correlations beyond the crossover regime, see Fig. 2. Our data cover five decades in time and more than five orders of magnitude in signal. The data clearly display an anti-correlated long-time tail

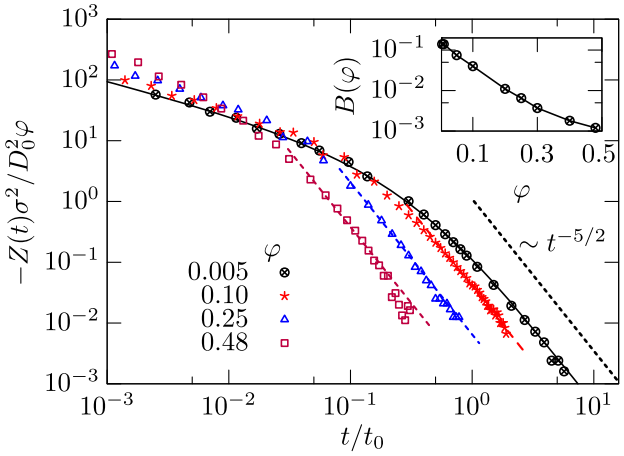

FIG. 2. Log-log plot of the reduced VACF of monodisperse Brownian hard spheres for increasing packing fraction φ. Symbols represent simulation data. The black solid line is the exact low-density expansion, Eq. (5). The colored dashed lines are fits to the power-law tails. The dashed black line labeled $t^{-5/2}$ is added as guide to the eye. Inset: Prefactor of the tail vs packing fraction.

$$Z(t) \simeq -\varphi B(\varphi) \frac{D_0^2}{\sigma^2} \left(\frac{t}{t_0}\right)^{-5/2}, \qquad t \to \infty, \tag{4}$$

for all packing fractions with the anticipated exponent $-5/2$ and dimensionless prefactor $\varphi B(\varphi)$. Since a nontrivial VACF arises only in the interacting system, we have included φ explicitly in the prefactor. Our simulation results show that $B(\varphi \to 0) \approx 0.14$ saturates for small packing fractions. For the lowest densities we compare to the exact analytical results [19–21]

$$Z(t) = -8\varphi \frac{D_0^2}{\sigma^2} \left\{ \sqrt{\frac{t_0}{2\pi t}} - \cos(4t/t_0)[1 - 2S(\sqrt{8t/\pi t_0})] + \sin(4t/t_0)[1 - 2C(\sqrt{8t/\pi t_0})] \right\}, \tag{5}$$

for the first-order in the low-density expansion. Here $S(\cdot)$ and $C(\cdot)$ denote the Fresnel integrals [34]. Our data nicely follow the theoretical prediction for $\varphi \lesssim 0.01$, in particular, they exhibit the long-time tail with exact prefactor $B(\varphi \to 0) = 3/(8\sqrt{2\pi})$. For larger packing fractions, the prefactor $B(\varphi)$ displays a strong density dependence beyond the low-density prediction, Fig. 2 (Inset). We find that the amplitude is suppressed by a factor of ≈ 110 upon approaching the freezing transition.

All simulation data also display a divergent short-time behavior $Z(t) \sim -t^{-1/2}$, $t \to 0$, which is a peculiarity of the hard-sphere interaction [35,36]; this discussion is deferred to the Supplemental Material [27].

Mode-coupling theory.—Numerical solutions of the colloidal MCT equations [37,38] for the self-motion and, in particular the MSD, have been developed earlier [39] and successfully compared to experiments [40–43] and simulations [44]. Thus, in principle the VACF can be obtained by taking derivatives as in Eq. (1). Yet, so far MCT equations relied on equidistant grids in wave number space and cannot properly resolve long-wavelength phenomena arising from a continuum of wave numbers.

Here we rely on the Zwanzig-Mori procedure [37,45,46] for an exact equation of motion for the VACF in terms of the irreducible memory kernel $\zeta^{(s)}(t)$ (the autocorrelation function of the fluctuating force with projected dynamics)

$$Z(t) + D_0^2\beta^2\zeta^{(s)}(t) + D_0\beta^2 \int_0^t \zeta^{(s)}(t-t')Z(t')dt' = 0, \tag{6}$$

for $t > 0$. Within MCT [38] the memory kernel is connected to the self-intermediate scattering functions of the collective $S(k,t)$ and self-motion $S^{(s)}(k,t)$ by an integral over all wave numbers

$$\beta^2\zeta^{(s)}(t) = \frac{n}{6\pi^2} \int_0^\infty dk k^4 c(k)^2 S(k,t) S^{(s)}(k,t), \tag{7}$$

where $c(k)$ is the direct correlation function [1]. The intermediate scattering functions $S(k,t), S^{(s)}(k,t)$ are required as input for the memory kernel $\zeta^{(s)}(t)$. Then the VACF follows by a numerical solution of Eq. (6). We solve numerically the standard MCT equations, yet to resolve the long-wavelength dynamics, we rely on a grid with logarithmic spacing, see Supplemental Material [27] for details.

The numerical results for the VACF within MCT display a long-time tail for all packing fractions, see Fig. 3. It is well-known that MCT overestimates the slowing-down or the structural relaxation. For comparison with the simulation results, the packing fractions in MCT have been chosen to match the suppression of diffusion obtained from simulation results. The overall shape of the VACF compares favorably to the simulation results, in particular, we reproduce the strong density dependence of the prefactor of the long-time tail. Nevertheless, it appears that the suppression of the tail is even more drastic in MCT than in simulations, see the inset of Fig. 3. The MCT results show a similar short-time divergence $t^{-1/2}$ for $t \to 0$ as the simulation data and the exact low-density result.

To gain further insight into how MCT encodes the tail we analyze the behavior of the equations analytically for low densities and for long and short times. In the low-density regime $c(k) \mapsto 4\pi[\sin(k\sigma) - k\sigma\cos(k\sigma)]/k^3$, the force kernel $\zeta^{(s)}(t)$, Eq. (7), simplifies and reproduces the weak-coupling approximation [47–50] (essentially second order perturbation in the interaction). Here the intermediate scattering functions have to be evaluated for the noninteracting system $S(k,t) \mapsto \exp(-D_0k^2t)$, $S^{(s)}(k,t) \mapsto \exp(-D_0k^2t)$. Then, for low densities one finds $Z(t) = -D_0^2\beta^2\zeta^{(s)}(t)$ from

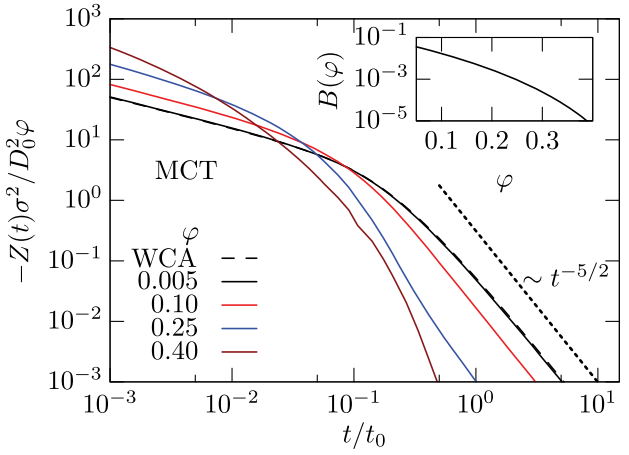

FIG. 3. Mode-coupling-theory results for the reduced VACF $Z(t)/\varphi$ for packing fraction φ with Percus-Yevick closure such that the diffusion coefficients match the simulation results. The short-dashed line indicates a power law $t^{-5/2}$ and serves as a guide to the eye. The long-dashed line corresponds to the weak-coupling approximation (w.c.a.) and is virtually on top of the MCT result for the lowest packing fraction. Inset: Prefactor of the tail vs packing fraction.

Eq. (6) for all times. The analytical result of the weak-coupling approximation is included in Fig. 3 and coincides with the numerical MCT solution for $\varphi \leq 0.005$. Interestingly, for the rather low packing fraction $\varphi = 0.10$, MCT yields already a long-time tail in $Z(t)/\varphi$ suppressed by a factor of 5, while in our simulations, $Z(t)/\varphi$ is suppressed by a factor of 4.

Mode-coupling theory provides an explanation for the origin of the tails similar to the classic hydrodynamic tails [3,4], which are due to transverse momentum conservation. In our case the coupling of the collective and self-intermediate scattering functions in the force, Eq. (7), yields a slowly decaying contribution for long wavelengths. For long times the integral is dominated by small wave numbers where the intermediate scattering functions $S(k,t) \simeq S(0)\exp[-D_0 k^2 t/S(0)]$, $S^{(s)}(k,t) \simeq \exp(-D^{(s)}k^2 t)$ approach diffusive motion. Here $D^{(s)}$ is again the long-time self-diffusion coefficient and $D_0/S(0)$ the collective diffusion coefficient (which is time-independent as a consequence of Newton's third law [48]). Then the MCT approximation yields a long-time tail $\zeta^{(s)}(t) \sim t^{-5/2}$ with a positive prefactor. The long-time behavior of the VACF $Z(t) \simeq -(D^{(s)})^2\beta^2\zeta^{(s)}(t)$ follows from the equation of motion, Eq. (6), using Tauber theorems. Collecting the prefactors yields the asymptotic long-time behavior for MCT:

$$Z(t) \simeq -(D^{(s)})^2 \frac{S(0)nc(0)^2/16\pi^{3/2}}{[D^{(s)} + D_0/S(0)]^{5/2}} t^{-5/2}. \qquad (8)$$

In particular, this yields a prediction for the low-density behavior with dimensionless amplitude $B(\varphi) = (1/6\sqrt{2\pi})$ consistent with the weak-coupling result [48]. Thus, the amplitude in weak-coupling is by a factor of $4/9$ smaller than the exact low-density expansion due to repeated encounters with the same scatterer.

It is interesting to ask how the long-time anomaly evolves with increasing density. At moderate packing fractions the fluid is barely compressible, $S(0) \ll 1$ (while $nc(0) = 1 - 1/S(0) \approx -1/S(0)$ via the Ornstein-Zernike relation [1]), hence the self-diffusion coefficient can be ignored in the denominator of Eq. (8) and the prefactor displays a strong $\sim S(0)^{3/2}$ dependence by mere compressibility effects. Upon changing the packing fraction from $\varphi = 0.005$ to $\varphi = 0.40$ the static structure factor $S(0)$ is suppressed by a factor of 24. Approaching the glass transition, the self-diffusion coefficient $D^{(s)}$ singularly goes to zero such that the tail in Eq. (8) becomes even more suppressed. At the same time the structural relaxation diverges and an intermediate window between the short-time anomaly and the long-time tail should open. Currently it appears to be unfeasible to test these predictions by simulations.

Summary and conclusion.—We have measured the VACF of an interacting colloidal system in Brownian dynamics simulations and observed an anti-correlated algebraic decay for long times. These underlying persistent correlations are masked in the MSD since the diffusive increase usually dominates. Therefore we have elaborated a novel algorithm that is sensitive only to the collisions, thereby enhancing the signal-to-noise ratio at least by an order of magnitude. The amplitude of the tail decreases by several orders of magnitude as the packing fraction is increased, which is qualitatively reproduced by MCT. The origin of the tail is also rationalized by MCT as a result of coupling of two slow diffusive modes.

While the low-density expansion is valid only up to packing fractions $\varphi \lesssim 0.01$, MCT provides a prediction for all densities, in particular, it predicts the strong suppression of the amplitude by static compressibility effects as well as by the slowing down of self-diffusion. MCT also generalizes the weak-coupling approximation where the direct correlation function is replaced by the bare interaction potential, $c(k) \mapsto -\beta u(k)$. This replacement arises also in a factorization of Gaussian fluctuations [51,52] but can be avoided in diagrammatic approaches [53]. Generally, the tails should also be present in modified MCT approaches [54–60]. Similar persistent correlations are anticipated also for the time-dependent stress-stress correlation functions, which determines the frequency-dependent shear modulus also encoded in the MCT approach.

In Brownian dynamics the solvent exerts friction only on the single-colloid level while hydrodynamic interactions (HI) can be accounted for in Stokesian dynamics simulations [61]. The low-density prediction [19–21] has been generalized to incorporate HI and display the same long-time tail $t^{-5/2}$, albeit with a somewhat corrected prefactor

[62]. Similarly, MCT including HI [49,50] merely modifies the vertex thereby affecting only the prefactor of the tail. For high densities HI are believed not to be crucial to understand the slow structural relaxation [63]. The tail appears also in the case of quenched disorder [55,64], such as in the Lorentz gas explored by a Brownian tracer as predicted in a low-density expansion [65] and was confirmed in Brownian dynamics simulations in 2D [66]. Therefore, one anticipates that the emergence of the tail should be a universal feature for any dynamics conserving only the particle number [67].

Noise-suppression algorithms relying on identical noise histories have been introduced before, mainly in nonequilibrium Brownian dynamics [68,69]. There, the equilibrium fluctuations are subtracted to enhance the signal for the average response for small driving which otherwise is dominated by fluctuations. The method proposed in our Letter is somewhat different, rather it addresses the interactions of the particles and remains applicable even at long times.

Our method of noise suppression by decomposing the displacements into a noninteracting contribution and a collision-induced one is not restricted to hard spheres (see Supplemental Material [27] for the simulation results for soft spheres) and should apply also in the case of confinement such as porous media [55,64]. Similarly, the strategy should be applicable also beyond the mean-square displacement upon introducing covariances of fluctuating intermediate scattering functions, similar to the measures of dynamic heterogeneities in glassy relaxations [70–73]. Then, subtle dynamical correlations in Brownian systems that are usually covered by the random fluctuations of the noninteracting system become accessible in simulations. Finally, nonequilibrium simulation setups to probe the nonlinear response should also be feasible with the noise-suppression algorithm.

We gratefully acknowledge Thomas Voigtmann for inspiring discussions and Rolf Schilling for a critical reading of the manuscript. This work has been supported by the Deutsche Forschungsgemeinschaft DFG via the Research Unit FOR1394 "Nonlinear Response to Probe Vitrification" and the Project No. LO 418/23-1 and by the Austrian Science Fund (FWF): I 2887.

[1] J. P. Hansen and I. R. McDonald, *Theory of Simple Liquids: with Applications to Soft Matter* (Academic Press, Amsterdam, 2013), 4th ed.

[2] B. J. Alder and T. E. Wainwright, Velocity Autocorrelations for Hard Spheres, Phys. Rev. Lett. **18**, 988 (1967); Decay of the velocity autocorrelation function, Phys. Rev. A **1**, 18 (1970).

[3] M. H. Ernst, E. H. Hauge, and J. M. J. van Leeuwen, Asymptotic Time Behavior of Correlation Functions, Phys. Rev. Lett. **25**, 1254 (1970).

[4] J. R. Dorfman and E. G. D. Cohen, Velocity Correlation Functions in Two and Three Dimensions, Phys. Rev. Lett. **25**, 1257 (1970).

[5] B. Lukić, S. Jeney, C. Tischer, A. J. Kulik, L. Forró, and E.-L. Florin, Direct Observation of Nondiffusive Motion of a Brownian Particle, Phys. Rev. Lett. **95**, 160601 (2005).

[6] S. Jeney, B. Lukić, J. A. Kraus, T. Franosch, and L. Forró, Anisotropic Memory Effects in Confined Colloidal Diffusion, Phys. Rev. Lett. **100**, 240604 (2008).

[7] T. Franosch, M. Grimm, M. Belushkin, F. M. Mor, G. Foffi, L. Forró, and S. Jeney, Resonances arising from hydrodynamic memory in Brownian motion, Nature (London) **478**, 85 (2011).

[8] R. Huang, I. Chavez, K. M. Taute, B. Lukić, S. Jeney, M. G. Raizen, and E.-L. Florin, Direct observation of the full transition from ballistic to diffusive Brownian motion in a liquid, Nat. Phys. **7**, 576 (2011).

[9] D. Lesnicki, R. Vuilleumier, A. Carof, and B. Rotenberg, Molecular Hydrodynamics from Memory Kernels, Phys. Rev. Lett. **116**, 147804 (2016).

[10] H. L. Peng, H. R. Schober, and Th. Voigtmann, Velocity autocorrelation function in supercooled liquids: Long-time tails and anomalous shear-wave propagation, Phys. Rev. E **94**, 060601(R) (2016).

[11] B. U. Felderhof, Effect of the wall on the velocity autocorrelation function and long-time tail of Brownian motion, J. Phys. Chem. B **109**, 21406 (2005).

[12] K. Huang and I. Szlufarska, Effect of interfaces on the nearby Brownian motion, Nat. Commun. **6**, 8558 (2015).

[13] D. Frenkel, Velocity auto-correlation functions in a 2d lattice Lorentz gas: Comparison of theory and computer simulation, Phys. Lett. **121A**, 385 (1987).

[14] S. R. Williams, G. Bryant, I. K. Snook, and W. van Megen, Velocity Autocorrelation Functions of Hard-Sphere Fluids: Long-Time Tails upon Undercooling, Phys. Rev. Lett. **96**, 087801 (2006).

[15] F. Höfling and T. Franosch, Crossover in the Slow Decay of Dynamic Correlations in the Lorentz Model, Phys. Rev. Lett. **98**, 140601 (2007).

[16] A. Fiege, T. Aspelmeier, and A. Zippelius, Long-Time Tails and Cage Effect in Driven Granular Fluids, Phys. Rev. Lett. **102**, 098001 (2009); I. Gholami, A. Fiege, and A. Zippelius, Slow dynamics and precursors of the glass transition in granular fluids, Phys. Rev. E **84**, 031305 (2011).

[17] R. Zwanzig and M. Bixon, Hydrodynamic theory of the velocity correlation function, Phys. Rev. A **2**, 2005 (1970).

[18] A. Widom, Velocity fluctuations of a hard-core Brownian particle, Phys. Rev. A **3**, 1394 (1971).

[19] S. Hanna, W. Hess, and R. Klein, The velocity autocorrelation function of an overdamped Brownian system with hard-core intraction, J. Phys. A **14**, L493 (1981); Self-diffusion of spherical Brownian particles with hard-core interaction, Physica (Amsterdam) **111A**, 181 (1982).

[20] B. J. Ackerson and L. Fleishman, Correlations for dilute hard core suspensions, J. Chem. Phys. **76**, 2675 (1982).

[21] B. Felderhof and R. Jones, Cluster expansion of the diffusion kernel of a suspension of interacting Brownian particles, Physica (Amsterdam) **121A**, 329 (1983); Diffusion in hard sphere suspensions, Physica (Amsterdam) **122A**, 89 (1983).

[22] B. Cichocki and B. U. Felderhof, Time-dependent self-diffusion coefficient of interacting Brownian particles, Phys. Rev. A **44**, 6551 (1991).
[23] A. Scala, Th. Voigtmann, and C. De Michele, Event-driven Brownian dynamics for hard spheres, J. Chem. Phys. **126**, 134109 (2007).
[24] P. Strating, Brownian dynamics simulation of a hard-sphere suspension, Phys. Rev. E **59**, 2175 (1999).
[25] Y.-G. Tao, W. K. den Otter, J. K. G. Dhont, and W. J. Briels, Isotropic-nematic spinodals of rigid long thin rodlike colloids by event-driven Brownian dynamics simulations, J. Chem. Phys. **124**, 134906 (2006).
[26] S. Leitmann, S. Mandal, M. Fuchs, A. M. Puertas, and T. Franosch, Time-dependent active microrheology in dilute colloidal suspensions, Phys. Rev. Fluids **3**, 103301 (2018).
[27] See Supplemental Material at http://link.aps.org/supplemental/10.1103/PhysRevLett.123.168001 for details on the logarithmic grid for MCT calculations, closure relations, smooth potentials, and compressibility effects, which included Refs. [28–33].
[28] F. J. Rogers and D. A. Young, New, thermodynamically consistent, integral equation for simple fluids, Phys. Rev. A **30**, 999 (1984).
[29] M. Heinen, P. Holmqvist, A. J. Banchio, and G. Nägele, Pair structure of the hard-sphere Yukawa fluid: An improved analytic method versus simulations, Rogers-Young scheme, and experiment, J. Chem. Phys. **134**, 044532 (2011).
[30] M. Heinen, E. Allahyarov, and H. Löwen, Highly asymmetric electrolytes in the primitive model: Hypernetted chain solution in arbitrary spatial dimensions, J. Comput. Chem. **35**, 275 (2014).
[31] R. Tough, P. Pusey, H. Lekkerkerker, and C. V. D. Broeck, Stochastic descriptions of the dynamics of interacting Brownian particles, Mol. Phys. **59**, 595 (1986).
[32] J. D. Weeks, D. Chandler, and H. C. Andersen, Role of repulsive forces in determining the equilibrium structure of simple liquids, J. Chem. Phys. **54**, 5237 (1971).
[33] J. A. Bollinger, J. Carmer, A. Jain, and T. M. Truskett, Impact of solvent granularity and layering on tracer hydrodynamics in confinement, Soft Matter **12**, 9561 (2016).
[34] *NIST Handbook of Mathematical Functions*, edited by F. W. J. Olver, D. W. Lozier, R. F. Boisvert, and C. W. Clark (Cambridge University Press, New York, NY, 2010); DLMF, NIST Digital Library of Mathematical Functions, http://dlmf.nist.gov/, Release 1.0.15 of 2017-06-01.
[35] B. Cichocki and B. Felderhof, Dynamic scattering function of a dense suspension of hard spheres, Physica (Amsterdam) **204A**, 152 (1994).
[36] A. J. Banchio, G. Nägele, and J. Bergenholtz, Collective diffusion, self-diffusion and freezing criteria of colloidal suspensions, J. Chem. Phys. **113**, 3381 (2000).
[37] G. Szamel and H. Löwen, Mode-coupling theory of the glass transition in colloidal systems, Phys. Rev. A **44**, 8215 (1991).
[38] W. Götze, *Complex Dynamics of Glass-Forming Liquids:A Mode-Coupling Theory* (Oxford University Press, Oxford, 2009).
[39] M. Fuchs, W. Götze, and M. R. Mayr, Asymptotic laws for tagged-particle motion in glassy systems, Phys. Rev. E **58**, 3384 (1998).
[40] W. van Megen, T. C. Mortensen, S. R. Williams, and J. Müller, Measurement of the self-intermediate scattering function of suspensions of hard spherical particles near the glass transition, Phys. Rev. E **58**, 6073 (1998).
[41] M. Sperl, Nearly logarithmic decay in the colloidal hard-sphere system, Phys. Rev. E **71**, 060401(R) (2005).
[42] Th. Voigtmann, Dynamics of colloidal glass-forming mixtures, Phys. Rev. E **68**, 051401 (2003).
[43] S. R. Williams and W. van Megen, Motions in binary mixtures of hard colloidal spheres: Melting of the glass, Phys. Rev. E **64**, 041502 (2001).
[44] Th. Voigtmann, A. M. Puertas, and M. Fuchs, Tagged-particle dynamics in a hard-sphere system: Mode-coupling theory analysis, Phys. Rev. E **70**, 061506 (2004).
[45] B. Cichocki and W. Hess, On the memory function for the dynamic structure factor of interacting Brownian particles, Physica (Amsterdam) **141A**, 475 (1987).
[46] K. Kawasaki, Irreducible memory function for dissipative stochastic systems with detailed balance, Physica (Amsterdam) **215A**, 61 (1995).
[47] J. A. Marqusee and J. M. Deutch, Concentration dependence of the self-diffusion coefficient, J. Chem. Phys. **73**, 5396 (1980).
[48] J. K. Dhont, *An Introduction to Dynamics of Colloids* (Elsevier, Amsterdam, 1996).
[49] G. Nägele, On the dynamics and structure of charge-stabilized suspensions, Phys. Rep. **272**, 215 (1996).
[50] G. Nägele and J. K. G. Dhont, Tracer-diffusion in colloidal mixtures: A mode-coupling scheme with hydrodynamic interactions, J. Chem. Phys. **108**, 9566 (1998).
[51] E. Zaccarelli, G. Foffi, F. Sciortino, P. Tartaglia, and K. A. Dawson, Gaussian density fluctuations and mode coupling theory for supercooled liquids, Europhys. Lett. **55**, 157 (2001).
[52] J. Wu and J. Cao, Gaussian factorization of hydrodynamic correlation functions and mode-coupling memory kernels, Phys. Rev. E **67**, 061116 (2003).
[53] G. Szamel, Dynamics of interacting Brownian particles: A diagrammatic formulation, J. Chem. Phys. **127**, 084515 (2007); Mode-coupling theory and beyond: A diagrammatic approach, Prog. Theor. Exp. Phys. **2013** 012J01 (2013).
[54] L. Yeomans-Reyna, M. A. Chávez-Rojo, P. E. Ramírez-González, R. Juárez-Maldonado, M. Chávez-Páez, and M. Medina-Noyola, Dynamic arrest within the self-consistent generalized Langevin equation of colloid dynamics, Phys. Rev. E **76**, 041504 (2007).
[55] T. Konincks and V. Krakoviack, Dynamics of fluids in quenched-random potential energy landscapes: A mode-coupling theory approach, Soft Matter **13**, 5283 (2017); V. Krakoviack, Statistical mechanics of homogeneous partly pinned fluid systems, Phys. Rev. E **82**, 061501 (2010); Liquid-Glass Transition of a Fluid Confined in a Disordered Porous Matrix: A Mode-Coupling Theory, Phys. Rev. Lett. **94**, 065703 (2005).
[56] J. Wu and J. Cao, High-Order Mode-Coupling Theory for the Colloidal Glass Transition, Phys. Rev. Lett. **95**, 078301 (2005).
[57] L. M. C. Janssen and D. R. Reichman, Microscopic Dynamics of Supercooled Liquids from First Principles, Phys. Rev. Lett. **115**, 205701 (2015); L. M. C. Janssen, P. Mayer, and D. R. Reichman, Relaxation patterns in supercooled

liquids from generalized mode-coupling theory, Phys. Rev. E **90**, 052306 (2014).

[58] M. K. Nandi, A. Banerjee, C. Dasgupta, and S. M. Bhattacharyya, Role of the Pair Correlation Function in the Dynamical Transition Predicted by Mode Coupling Theory, Phys. Rev. Lett. **119**, 265502 (2017).

[59] C. Contreras Aburto and G. Nägele, A unifying mode-coupling theory for transport properties of electrolyte solutions. I. General scheme and limiting laws, J. Chem. Phys. **139**, 134109 (2013).

[60] A. J. Banchio, M. Heinen, P. Holmqvist, and G. Nägele, Short- and long-time diffusion and dynamic scaling in suspensions of charged colloidal particles, J. Chem. Phys. **148**, 134902 (2018).

[61] J. F. Brady and G. Bossis, Stokesian dynamics, Annu. Rev. Fluid Mech. **20**, 111 (1988).

[62] R. Jones and G. Burfield, Memory effects in the diffusion of an interacting polydisperse suspension: II. Hard spheres at low density, Physica (Amsterdam) **111A**, 577 (1982).

[63] G. L. Hunter and E. R. Weeks, The physics of the colloidal glass transition, Rep. Prog. Phys. **75**, 066501 (2012).

[64] G. Pellicane, C. Caccamo, D. S. Wilson, and L. L. Lee, Replica Ornstein-Zernike self-consistent theory for mixtures in random pores, Phys. Rev. E **69**, 061202 (2004).

[65] T. Franosch, F. Höfling, T. Bauer, and E. Frey, Persistent memory for a Brownian walker in a random array of obstacles, Chem. Phys. **375**, 540 (2010).

[66] T. Bauer, F. Höfling, T. Munk, E. Frey, and T. Franosch, The localization transition of the two-dimensional Lorentz model, Eur. Phys. J. Spec. Top. **189**, 103 (2010).

[67] H. van Beijeren, Transport properties of stochastic Lorentz models, Rev. Mod. Phys. **54**, 195 (1982).

[68] H. C. Oettinger, Variance reduced Brownian dynamics simulations, Macromolecules **27**, 3415 (1994); M. Melchior and H. C. Öttinger, Variance reduced simulations of polymer dynamics, J. Chem. Phys. **105**, 3316 (1996); N. J. Wagner and H. C. Öttinger, Accurate simulation of linear viscoelastic properties by variance reduction through the use of control variates, J. Rheol. **41**, 757 (1997).

[69] D. J. Evans and G. Morriss, *Statistical Mechanics of Nonequilibrium Liquids* (Cambridge University Press, Cambridge, England, 2008).

[70] S. C. Glotzer, V. N. Novikov, and T. B. Schrøder, Time-dependent, four-point density correlation function description of dynamical heterogeneity and decoupling in supercooled liquids, J. Chem. Phys. **112**, 509 (2000).

[71] E. Flenner and G. Szamel, Dynamic Heterogeneity in a Glass Forming Fluid: Susceptibility, Structure Factor, and Correlation Length, Phys. Rev. Lett. **105**, 217801 (2010); E. Flenner, M. Zhang, and G. Szamel, Analysis of a growing dynamic length scale in a glass-forming binary hard-sphere mixture, Phys. Rev. E **83**, 051501 (2011).

[72] L. Berthier, G. Biroli, J.-P. Bouchaud, L. Cipelletti, and W. van Saarloos, *Dynamical Heterogeneities in Glasses, Colloids, and Granular Media* (Oxford University Press, Oxford, 2011).

[73] K. E. Avila, H. E. Castillo, A. Fiege, K. Vollmayr-Lee, and A. Zippelius, Strong Dynamical Heterogeneity and Universal Scaling in Driven Granular Fluids, Phys. Rev. Lett. **113**, 025701 (2014).